Optimization in Prostate Cancer Detection

Ariela Sofer[1], Jianchao Zeng[2], and Seong K. Mun[2]

[1] Department of Systems Engineering and Operations Research
George Mason University, Fairfax, VA 22030
asofer@gmu.edu
http://www.gmu.edu/departments/ore/sofer.html
[2] Imaging Science and Information Systems Center (ISIS)
Department of Radiology, Georgetown University Medical Center
zeng@isis.imac.georgetown.edu (J. Zeng)
http://www.simulation.georgetown.edu

Abstract. Clinical diagnosis of prostate cancer is most often done by transrectal ultrasound-guided needle biopsy. Because of the low resolution of ultrasound, however, the urologist cannot usually distinguish between cancerous and healthy tissue. Therefore, most biopsies follow standard protocols based on long-term physician experience. Recent studies indicate that these protocols may have a significant rate of false negative diagnoses. This research develops optimized biopsy protocols. We use real prostate specimens removed by prostatectomy to develop a 3D distribution map of cancer in the prostate. We develop also a probability model of the needle insertion procedure. Using this model, the tumor map, and the geometry of the biopsy needle, we obtain estimates for the probability of obtaining a positive biopsy in various zones of prostates with cancer. We develop a nonlinear optimization problem that determines the protocols that maximize the probability of cancer detection for a given number of needles, and present new optimized protocols.

1 Introduction

Prostate cancer is the most prevalent male malignancy and the second leading cause of death by cancer in American men. The American Cancer Society estimates that there will be about 198,100 new cases of prostate cancer in the United States in 2001, and about 32,000 men will die of the disease. Current screening for the cancer includes the prostate specific antigen (PSA) test and the digital rectal exam. However the cancer can only be correctly diagnosed by needle biopsy of the prostate and histopathology of the sampled tissues. The most common technique for detection of prostate cancer is transrectal ultrasound-guided (TRUS) needle core biopsy.

Since normal prostate tissue cannot usually be differentiated from cancerous tissue during the biopsy, a number of standard protocols have been developed to assist the urologist in performing the biopsy. The protocol most commonly used is the systematic sextant biopsy [4]. Recent studies [1], [7] have shown, however, that this strategy has an unacceptable level of false negative diagnoses, and that

W. Niessen and M. Viergever (Eds.): MICCAI 2001, LNCS 2208, pp. 1114–1121, 2001.

many patients who have a negative initial biopsy are found to have cancer in repeat biopsies.

As a result, recent clinical studies have investigated new protocols that have higher detection rates [2], [3]. The improvement in detection is obtained by using additional needles (up to seven more) in the biopsy.

Our approach is different: our goal is to develop optimized biopsy protocols. For a specified number of needles, an optimal protocol is one that maximizes the probability of detection of cancer in a patient. The hope is that with optimized protocols one could achieve improved detection rates with fewer needles.

A major component of our effort is the development of a statistical distribution map of cancer in the prostate. The map is constructed from cancerous prostates that were removed via prostatectomy. Each of the prostates is first reconstructed into a 3D computerized model that accurately represent the anatomy of the prostate, and the distribution of cancer within it. Next, each model is divided into zones based on clinical conventions, and the presence of cancer in each zone is calculated. From this the 3D distribution map of tumor location is developed. Thus far, 301 prostates have been reconstructed and analyzed.

We have previously established a statistical distribution map and optimal biopsy protocols for a 48-zone division of the prostate [8], [10]. The rationale for the division is that it is likely the upper limit on the number of zones that can still be accessible by the physician. A drawback of the model, however, is that it assumes that a biopsy taken in a cancerous zone is bound to be positive. In practice, it is possible that a biopsy in a cancerous zone will be negative.

In this paper we address this issue. Although we still maintain a coarse grid (i.e., the 48-zone division) for the purpose of biopsy guidance for the physician, we use a much finer grid for the development of a cancer distribution map. Each of the 48 zones is thus further divided to a larger number of subzones, with each subzone smaller in volume (and sometimes much smaller) than the needle core size. The presence of cancer is evaluated in each subzone to create a fine-grid cancer distribution map. This information is then used to estimate, for each patient, the probability that a biopsy in a given zone will be positive, and in turn, the probability that a given biopsy protocol will detect cancer. This leads to more accurate estimates of detection rates, and improved biopsy protocols.

2 Reconstruction of the Prostate Models and Statistical Distribution Map

The reconstruction of the prostates involved several steps [9]. Each prostate was sectioned in 4μm sections at 2.25mm intervals, and each slice was digitized with a scanning resolution of 1500 dots per inch. Each digitized image was segmented by a pathologist to identify the key pathological structures, including surgical margins, capsule, urethra, seminal vesicle, and the tumor. The contours of each structure were identified on each slice, and then stacked up. Interpolation between pairs of contours was performed using a 3D elastic contour model. The 3D

model of each structure in the prostate was finalized by tiling triangular patches onto the interpolated contours, using a deformable surface-spine model.

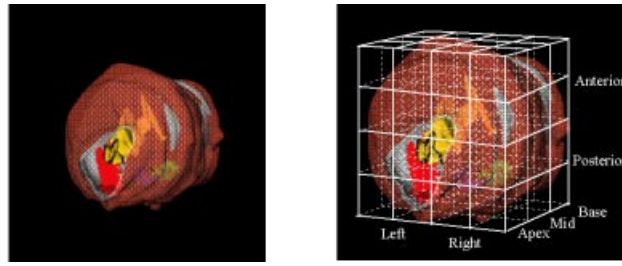

(a) (b)

Fig. 1. Figure 1: 3D reconstruction of prostate models: (a) Final 3D reconstructed prostate model. (b) 48-zone grid superimposed over prostate.

Next we determine the statistical distribution map. The coarse grid 48-zone coarse grid used for biopsy guidance is illustrated in Figure 1. The grid has three transverse layers, base, mid, and apex. Each such layer is further divided into four coronal layers, which, following clinical conventions, are labeled from the posterior to the anterior as posterior 1, posterior 2, anterior 1, and anterior 2 respectively. Finally, the layers are divided from left to right into four sagittal layers, denoted as left lateral, left mid, right mid, and right lateral, respectively. It is noted that the size of the zones will vary with the size of a prostate model. A larger prostate model ends up with having a larger size for each of its 48 zones. This variation of zone sizes is the natural and consistent reflection of the original prostate, and it should not affect the accuracy of cancer distributions.

For determination of the statistical distribution map, each of the course-grid compartments is further divided to smaller subzones. We have used a total of 5^3 subzones per zone, so that the final grid superimposed over the prostate has 6000 subzones. The occurrence of cancer is calculated in each of the subzones for each of the patients; a subzone is considered positive for a given patient if it contains any part of a cancer. Subzones that contain no prostate tissue are marked accordingly.

Next, we estimate for each patient and for each of the coarse-grid zones, the probability that a needle biopsy in the zone will detect cancer. To ensure accuracy we will model the variability in the physician's placement of the needle. Specifically for each of the 48 zones we model (i) the depth of the needle insertion point (from apex to base); (ii) the longitudinal position of the needle insertion point (from posterior to anterior) and (iii) the firing angle of the needle. (Note that the physician controls the firing angle by rotating the ultrasound probe around its axis; there is only one degree of freedom, since the needle has a fixed angle with respect to the axis of the ultrasound probe.) We now assume that

for each zone the three corresponding random variables controlling the needle trajectory are statistically independent Gaussian variables. (The parameters of these distributions will vary from zone to zone.) We then use a discretization of these distributions, to estimate for each patient, the probability that a needle probe in the zone will be positive. The analysis is based on the fine-grid cancer distribution map, the volume of each subzone, the geometry of the needle and the volume of the needle core.

3 The Optimization Problem

3.1 Problem Formulation

We now develop a mathematical model that determines the optimal locations for the biopsy needles based on the 3D cancer distribution model. The objective is to determine, for a specified number of needles, the protocol that maximizes the probability of detecting cancer. We note that while the detection rate increases with the number of needles, using optimized strategies could permit using fewer needles, thus avoiding patient discomfort and saving costs.

To formulate the problem, let n denote the number of zones in the coarse grid (here $n = 48$), and let m denote the number of patients in our sample ($m = 301$). Define variables x_j, $j = 1, \ldots, n$, by

$$x_j = \begin{cases} 1 \text{ if a biopsy is taken in zone } j, \\ 0 \text{ otherwise.} \end{cases}$$

Let p_{ij} be the estimated probability that a needle in zone j will detect cancer in patient i ($i = 1, \ldots, m$, $j = 1, \ldots, n$), and let $q_{ij} = 1 - p_{ij}$. We have that

$$(q_{ij})^{x_j} = \begin{cases} 1 & \text{if } x_j = 0 \\ q_{ij} & \text{if } x_j = 1. \end{cases}$$

Now in general, the occurrence of cancer in adjacent prostate zones is correlated. But for a given patient i in our sample the location of cancer is known, hence the occurrence of cancer is no longer a random variable (but its realization). In contrast, the outcome of a needle biopsy in a given zone for this patient is a random variable. The randomness is due only to the uncertainty in how the physician places the needle; if the placement of the needle were totally deterministic, the outcome of the needle biopsy would also be deterministic. Since the physician's positioning of different needles can be assumed to be statistically independent, the outcomes of needle biopsies in different zones can be assumed to be statistically independent. Thus the probability that a set of needle biopsies diagnoses cancer in patient i of our sample is

$$1 - \prod_{j=1}^{n} (q_{ij})^{x_j}.$$

It follows that the k-needle biopsy protocol that maximizes the probability of detection for a randomly selected patient in our sample solves

$$\begin{aligned} \text{maximize } & \frac{1}{m}\sum_{i=1}^{m}(1-\prod_{j=1}^{n}(q_{ij})^{x_j}) \\ \text{subject to } & \sum_{j=1}^{n}x_j = k \\ & x_j \in \{0,1\} \end{aligned} \tag{1}$$

Note that when scaled by m, the objective function is the expected number of patients in the sample to be diagnosed with cancer. Problem (1) can be written equivalently as

$$\begin{aligned} \text{minimize } & \sum_{i=1}^{m}\prod_{j=1}^{n}(q_{ij})^{x_j} \\ \text{subject to } & \sum_{j=1}^{n}x_j = k \\ & x_j \in \{0,1\} \end{aligned} \tag{2}$$

Additional constraints reflecting physician preferences can also be added. For example, left-right symmetry of the protocols is obtained by the constraints $x_l = x_r$ for every pair of zones l and r that are left-right symmetric. One may also restrict biopsies to zones in the posterior area (since the anterior is more difficult to probe), by imposing the constraint $x_a = 0$ for all zones a in the anterior. For simplicity we will let X denote the feasible set—the set of vectors $x \in \{0,1\}$ that satisfy $\sum_{j=1}^{n} x_j = k$ and any additional desired constraint.

The optimization problem (2) is a nonlinear integer problem. In its current form the problem is difficult to solve, since its objective is a nonconvex function in the integer variables x_j. However we can transform it to a more tractable problem. Let ϵ be some (sufficiently) small positive tolerance (say, $\epsilon = 10^{-10}$), and define the $m \times n$ matrix U by $u_{ij} = -\log(\max\{q_{ij}, \epsilon\})$. Denoting $z_i = \sum_{j=1}^{n} u_{ij}x_j$, the optimization problem is equivalent to the problem

$$\begin{aligned} \text{minimize } & \sum_{i=1}^{m} e^{-z_i} \\ \text{subject to } & z - Ux = 0 \\ & x \in X \end{aligned} \tag{3}$$

Although the resulting problem is still nonlinear and integer, the transformed form is more convenient, since the objective function is convex.

3.2 Solution of the Optimization Problem

To solve problem (3) we use a generalized decomposition algorithm [6] framework. The idea is to decompose the problem in a way that enables the creation of

a sequence of easier subproblems that gradually provide tighter lower and upper bounds on the optimal objective. Here this is done as follows: We rewrite (3) as

$$\underset{x\in X}{\text{minimize}} \underbrace{\begin{array}{ll} \min\limits_{z} & g(z) = \sum e^{-z_i} \\ \text{subject to} & z - Ux = 0 \end{array}}_{\text{primal problem}} \tag{4}$$

Let $L(x,\lambda) = \sum_{i=1}^{m} e^{-z_i} - \lambda^T(z - Ux)$ be the Lagrangian for the primal problem. Now because the problem is convex, its objective is equal to that of its Lagrangian dual [6]. Hence (4) is equivalent to

$$\underset{x\in X}{\text{minimize}} \quad \max_{\lambda} \min_{z} \left(\sum e^{-z_i} - \lambda^T(z - Ux)\right). \tag{5}$$

Problem (5) can be written in equivalent form

$$\begin{array}{ll} \underset{x\in X,\delta}{\text{minimize}} & \delta \\ & \delta \geq \min\limits_{z}(\sum e^{-z_i} - \lambda^T(z - Ux)) \quad \forall\lambda \end{array}$$

Suppose we start from an initial feasible integer point x^0. It is easy to show that for a given vector x^t, the solution to the primal problem in (4) is

$$z^t = Ux^t \quad \lambda_i^t = -e^{-z_i^t}.$$

This yields at iteration t an upper bound UB=min$\{UB, g(x^t\}$ on the optimal objective, where at iteration 0, UB=$g(z^0)$. Now given the iterates $x^0, \ldots, x^t$, the problem

$$\begin{array}{ll} \underset{x\in X,\delta}{\text{minimize}} & \delta \\ & \delta \geq (\lambda^j)^T Ux + \sum e^{-z_i^j} - (\lambda^j)^T z^j, \quad j = 0, \ldots, t \end{array}$$

is a "relaxation" of Problem 3.2, in the sense that it relaxes its constraints. Thus the solution provides a lower bound on the optimal objective LB=δ and a new starting x^{t+1} for the primal.

We can thus obtain a sequence of solutions to the primal problem and the dual problem, with the former yielding a nonincreasing sequence of upper bounds to the optimal objective value, and the latter yielding a nondecreasing sequence of lower bounds to this objective value. The algorithm terminates when the upper and lower bounds differ by less than a prescribed tolerance. The relaxed dual problems are linear programs with integer variables, and are easily solved by the software package ILOG CPlex 6.5 [5].

4 Optimized Protocols

We have obtained some preliminary results using the sample of 301 prostate analyzed so far. The resulting estimated detection rates for optimized 6-, 8-, and

10-needle biopsy protocols are shown in Table 1. As one can see, the estimated detection rate for our optimal 6-needle protocols is about 79%. In contrast, the estimated detection rate for the sextant method is about 67%. Thus it is possible to improve detection rates with 6 needles only, just by using optimized protocols. Additional needles will further improve the detection rates as indicated in the Table. The corresponding optimal biopsy protocols are shown in Table 2.

Table 1. Estimated detection rates with optimized symmetric protocols using 6, 8, and 10 needles. Estimated detection rate for sextant method is 67.3%

No. of Needles	Posterior Only	Entire Gland
6	78.8%	79.3%
8	81.6%	82.9%
10	84.2%	85.5%

5 Conclusions and Future Work

Preliminary results show that the optimal biopsy protocols have a substantial improvement over the protocols currently used clinically. Simulation using additional 100 prostate models is under way and initial results have also confirmed this improvement. A post-optimality sensitivity analysis will also be performed to assess the sensitivity of our solutions to the model's parameters.

A new generation of image-guided prostate biopsy system is now being developed. We are developing an image segmentation technique to acquire the boundary of a series of transverse ultrasound images of the prostate. These are used to construct a 3-D prostate surface model of the patient. The intersection of the ultrasound beam with the reconstructed 3-D model enables us to extract the corresponding cancer distribution information and optimized biopsy protocols and to superimpose the information onto the ultrasound image as highlighted grids. This information will significantly enhance the physicians' situation awareness and thus lead to a substantial improved performance of cancer detection.

Acknowledgements
Ariela Sofer is partially supported by National Science Foundation grant DMI-9800544. Jianchao Zeng is supported in part by The Whitaker Foundation Biomedical Engineering Program grant RG-99-0115. We wish to acknowledge the input of John J. Bauer (WRMC), Wei Zhang and Isabell A. Sesterhenn (AFIP), and Judd W. Moul (CPDR).

References

1. Bankhead C.: "Sextant biopsy helps in prognosis of Pca, but its not foolproof," Urology Times, Vol. 25, (1997) No. 8. (August).

Table 2. Optimal symmetric biopsy protocols for 6, 8, and 10 needles. x indicates a zone that is part of the biopsy; ll, lm, rm, and rl indicate left lateral, left mid, right mid, and right lateral respectively; p1, p2, a1, and a2 denote posterior 1 and 2, and anterior 1 and 2 respectively.

		Base				Mid				Apex			
		ll	lm	rm	rl	ll	lm	rm	rl	ll	lm	rm	rl
6 needles	a2												
	a1					x			x				
	p2										x	x	
	p1					x			x				
8 needles	a2												
	a1					x			x				
	p2	x			x						x	x	
	p1					x			x				
10 needles	a2												
	a1					x			x				
	p2	x			x						x	x	
	p1					x			x		x	x	

2. Chang J.J., Shinohara K., Bhargava V., Presti, J.C. Jr.: "Prospective evaluation of lateral biopsies of the peripheral zone for prostate cancer detection," J. Urology, Vol. 160, (1997), pp. 2111–2114.
3. Eskew, A.L., Bare,R.L., McCullough D.L.: "Systematic 5-region prostate biopsy is superior to sextant method for detecting carcinoma of the prostate." J. Urology, Vol. 157 (1997), pp. 199–202.
4. Hodge K.K, McNeal J.E., Terris M.K., and Stamey T.A.: "Random systematic versus directed ultrasound guided trans-rectal core biopsies of the prostate," J. Urology Vol. 142, (1989) pp. 71–74
5. ILOG CPLex 6.5 User Manual, ILOG, 1999.
6. Nash, S.G, and Sofer, A: Linear and Nonlinear Programming, McGraw Hill, 1996.
7. Rabbani F., Stroumbakis N., Kava B.R., Cookson M.S., and Fair W.R.: "Incidence and clinical significance of false-negtive sextant prostate biopsies," J. Urology Vol. 159 (1998), pp. 1247–1250.
8. Sofer, A., Zeng, J., Opell, B., Bauer, J., Mun, S.K., "Optimal Biopsy Protocols for Prostate Cancer," submitted for publication in Interfaces, October 2000.
9. Zeng, J., Bauer J.J., Yao X., Zhang W., Sesterhenn I.A., Connelly R.R., Moul J., and Mun S.K.: "Building an accurate 3D map of prostate cancer using computerized models of 280 whole-mounted radical prostatectomy specimens." Proc. of SPIE Medical Imaging Conference, Vol. 3976, 2000, pp. 466-477.
10. . Zeng, J., Bauer, J., Sofer, A., Yao, X., Opell, B., Zhang, W., Sestrehenn, I. A., Moul, J. W., Lynch, J., Mun, S. K.: Distribution of Prostate Cancer for Optimized Biopsy Protocols. In Proceedings of the Medical Image Computing and Computer Assisted Intervention Conference, 2000, pp. 287-296.